

World Journal of *Gastroenterology*

World J Gastroenterol 2020 September 14; 26(34): 5060-5222



REVIEW

- 5060 Transjugular intrahepatic portosystemic shunt for Budd-Chiari syndrome: A comprehensive review
Inchingolo R, Posa A, Mariappan M, Tibana TK, Nunes TF, Spiliopoulos S, Brountzos E
- 5074 Role of succinate dehydrogenase deficiency and oncometabolites in gastrointestinal stromal tumors
Zhao Y, Feng F, Guo QH, Wang YP, Zhao R

MINIREVIEWS

- 5090 Potential applications of artificial intelligence in colorectal polyps and cancer: Recent advances and prospects
Wang KW, Dong M

ORIGINAL ARTICLE**Basic Study**

- 5101 Arachidyl amido cholanoic acid improves liver glucose and lipid homeostasis in nonalcoholic steatohepatitis *via* AMPK and mTOR regulation
Fernández-Ramos D, Lopitz-Otsoa F, Delacruz-Villar L, Bilbao J, Pagano M, Mosca L, Bizkarguenaga M, Serrano-Macia M, Azkargorta M, Iruarizaga-Lejarreta M, Sot J, Tsvirkun D, van Liempd SM, Goni FM, Alonso C, Martínez-Chantar ML, Elortza F, Hayardeny L, Lu SC, Mato JM
- 5118 Acupuncture improved lipid metabolism by regulating intestinal absorption in mice
Han J, Guo X, Meng XJ, Zhang J, Yamaguchi R, Motoo Y, Yamada S

Retrospective Study

- 5130 Golgi protein-73: A biomarker for assessing cirrhosis and prognosis of liver disease patients
Gatselis NK, Tornai T, Shums Z, Zachou K, Saitis A, Gabeta S, Albesa R, Norman GL, Papp M, Dalekos GN
- 5146 Endoscopy-based Kyoto classification score of gastritis related to pathological topography of neutrophil activity
Toyoshima O, Nishizawa T, Yoshida S, Sakaguchi Y, Nakai Y, Watanabe H, Suzuki H, Tanikawa C, Matsuda K, Koike K
- 5156 Construction of a convolutional neural network classifier developed by computed tomography images for pancreatic cancer diagnosis
Ma H, Liu ZX, Zhang JJ, Wu FT, Xu CF, Shen Z, Yu CH, Li YM

Observational Study

- 5169 Experimental model standardizing polyvinyl alcohol hydrogel to simulate endoscopic ultrasound and endoscopic ultrasound-elastography
Galvis-García ES, Sobrino-Cossío S, Reding-Bernal A, Contreras-Marín Y, Solórzano-Acevedo K, González-Zavala P, Quispe-Siccha RM

SYSTEMATIC REVIEWS

- 5181** Mixed epithelial endocrine neoplasms of the colon and rectum – An evolution over time: A systematic review

Kanthan R, Tharmaradinam S, Asif T, Ahmed S, Kanthan SC

META-ANALYSIS

- 5207** Efficacy of pancreatoscopy for pancreatic duct stones: A systematic review and meta-analysis

Saghir SM, Mashiana HS, Mohan BP, Dhindsa BS, Dhaliwal A, Chandan S, Bhogal N, Bhat I, Singh S, Adler DG

LETTER TO THE EDITOR

- 5220** Peliosis hepatis complicated by portal hypertension following renal transplantation

Demyashkin G, Zatsepina M

ABOUT COVER

Editorial Board of *World Journal of Gastroenterology*, Dr. Rosa Leonôra Salerno Soares is Full Professor at the Faculty of Medicine of Universidade Federal Fluminense (Niterói, Rio de Janeiro). She completed her doctorate in medicine at the Federal University of Rio de Janeiro in 1994 and post-doctorate training in 2009 at the University of Porto, Portugal. Her career experience in internal medicine and clinical research is founded upon her interests in medicine, gastroenterology, intestinal diseases, functional diseases of the gastrointestinal tract, and nutritional support. Her academic teaching pursuits encompass curriculums in applying the scientific methodology to the health field. Currently, she is Head of the Department of Clinical Medicine (MMC) of the Faculty of Medicine of Universidade Federal Fluminense. Her full curriculum vitae can be accessed at: <http://lattes.cnpq.br/4236328959320774>. (L-Editor: Filipodia)

AIMS AND SCOPE

The primary aim of *World Journal of Gastroenterology* (*WJG*, *World J Gastroenterol*) is to provide scholars and readers from various fields of gastroenterology and hepatology with a platform to publish high-quality basic and clinical research articles and communicate their research findings online. *WJG* mainly publishes articles reporting research results and findings obtained in the field of gastroenterology and hepatology and covering a wide range of topics including gastroenterology, hepatology, gastrointestinal endoscopy, gastrointestinal surgery, gastrointestinal oncology, and pediatric gastroenterology.

INDEXING/ABSTRACTING

The *WJG* is now indexed in Current Contents®/Clinical Medicine, Science Citation Index Expanded (also known as SciSearch®), Journal Citation Reports®, Index Medicus, MEDLINE, PubMed, PubMed Central, and Scopus. The 2020 edition of Journal Citation Report® cites the 2019 impact factor (IF) for *WJG* as 3.665; IF without journal self cites: 3.534; 5-year IF: 4.048; Ranking: 35 among 88 journals in gastroenterology and hepatology; and Quartile category: Q2.

RESPONSIBLE EDITORS FOR THIS ISSUE

Production Editor: Yan-Liang Zhang; Production Department Director: Yun-Xiaojian Wu; Editorial Office Director: Ze-Mao Gong.

NAME OF JOURNAL

World Journal of Gastroenterology

ISSN

ISSN 1007-9327 (print) ISSN 2219-2840 (online)

LAUNCH DATE

October 1, 1995

FREQUENCY

Weekly

EDITORS-IN-CHIEF

Andrzej S Tarnawski, Subrata Ghosh

EDITORIAL BOARD MEMBERS

<http://www.wjgnet.com/1007-9327/editorialboard.htm>

PUBLICATION DATE

September 14, 2020

COPYRIGHT

© 2020 Baishideng Publishing Group Inc

INSTRUCTIONS TO AUTHORS

<https://www.wjgnet.com/bpg/gerinfo/204>

GUIDELINES FOR ETHICS DOCUMENTS

<https://www.wjgnet.com/bpg/GerInfo/287>

GUIDELINES FOR NON-NATIVE SPEAKERS OF ENGLISH

<https://www.wjgnet.com/bpg/gerinfo/240>

PUBLICATION ETHICS

<https://www.wjgnet.com/bpg/GerInfo/288>

PUBLICATION MISCONDUCT

<https://www.wjgnet.com/bpg/gerinfo/208>

ARTICLE PROCESSING CHARGE

<https://www.wjgnet.com/bpg/gerinfo/242>

STEPS FOR SUBMITTING MANUSCRIPTS

<https://www.wjgnet.com/bpg/GerInfo/239>

ONLINE SUBMISSION

<https://www.f6publishing.com>

Observational Study

Experimental model standardizing polyvinyl alcohol hydrogel to simulate endoscopic ultrasound and endoscopic ultrasound-elastography

Elymir S Galvis-García, Sergio Sobrino-Cossío, Arturo Reding-Bernal, Yesica Contreras-Marín, Karina Solórzano-Acevedo, Patricia González-Zavala, Rosa M Quispe-Siccha

ORCID number: Elymir S Galvis-García 0000-0002-1674-3664; Sergio Sobrino-Cossío 0000-0001-6093-1868; Arturo Reding-Bernal 0000-0003-4318-181X; Yesica Contreras-Marín 0000-0003-2879-5709; Karina Solórzano-Acevedo 0000-0002-7058-7439; Patricia González-Zavala 0000-0002-1330-5482; Rosa M Quispe-Siccha 0000-0003-1178-8529.

Author contributions: Quispe Siccha RM established the design and concept of the study; Galvis García ES and Sobrino Cossío S executed the figures; Quispe Siccha RM, González Zaval P, Contreras Marín Y and Solórzano Acevedo K provided and validated the PVA phantoms; Sobrino Cossío S, Galvis García ES, Reding Bernal A and Quispe Siccha RM analyzed data from the literature, and Reding Bernal A performed the statistical analysis; Sobrino Cossío S and Quispe Siccha RM edited the first draft of the manuscript, which was critically discussed and revised in terms of intellectual content by Galvis García ES and Reding Bernal A; all authors discussed the statement and conclusions and approved the final version for publication.

Elymir S Galvis-García, Unidad de Endoscopia Gastrointestinal, Hospital General de México "Dr. Eduardo Liceaga", Mexico 06720, Mexico

Sergio Sobrino-Cossío, Unidad de Endoscopia y Fisiología Digestiva, Hospital Ángeles del Pedregal, Mexico 10700, Mexico

Arturo Reding-Bernal, Dirección de Investigación, Hospital General de México "Dr. Eduardo Liceaga", Mexico 06720, Mexico

Yesica Contreras-Marín, Karina Solórzano-Acevedo, Unidad Profesional Interdisciplinaria de Biotecnología and Unidad de Investigación y Desarrollo Tecnológico, Instituto Politécnico Nacional and Hospital General de México "Dr. Eduardo Liceaga", Mexico 06720, Mexico

Patricia González-Zavala, Instituto de Investigaciones en Materiales and Unidad de Investigación y Desarrollo Tecnológico, Universidad Nacional Autónoma de México and Hospital General de México "Dr. Eduardo Liceaga", Mexico 06720, Mexico

Rosa M Quispe-Siccha, Unidad de Investigación y Desarrollo Tecnológico, Hospital General de México "Dr. Eduardo Liceaga", Mexico 06720, Mexico

Corresponding author: Rosa M Quispe-Siccha, PhD, Academic Research, Research Scientist, Unidad de Investigación y Desarrollo Tecnológico, Hospital General de México "Dr. Eduardo Liceaga", Dr. Balmis 148, Doctores, Cuauhtémoc, Mexico 06720, Mexico.
rosa.quispe@gmail.com

Abstract

BACKGROUND

Endoscopic ultrasound (EUS) and endoscopic ultrasound elastography (EUS-E) simulation lessens the learning curve; however, models lack realism, diminishing competitiveness.

AIM

To standardize the mechanical properties of polyvinyl alcohol (PVA) hydrogel for simulating organs and digestive lesions.

Institutional review board

statement: The study was reviewed and approved by the Science and Research Office of Hospital General de México “Dr. Eduardo Liceaga” (México) (Approval No. DI/12/11/04/017).

Informed consent statement:

Patient details on ultrasound/elastography images have been removed to ensure anonymity.

Conflict-of-interest statement:

There are no conflicts of interest to report.

Data sharing statement:

No additional data are available.

STROBE statement: The authors have read the STROBE Statement-checklist of items, and the manuscript was prepared and revised according to the STROBE Statement-checklist of items.

Open-Access: This article is an open-access article that was selected by an in-house editor and fully peer-reviewed by external reviewers. It is distributed in accordance with the Creative Commons Attribution NonCommercial (CC BY-NC 4.0) license, which permits others to distribute, remix, adapt, build upon this work non-commercially, and license their derivative works on different terms, provided the original work is properly cited and the use is non-commercial. See: <http://creativecommons.org/licenses/by-nc/4.0/>

Manuscript source: Unsolicited manuscript

Received: April 30, 2020

Peer-review started: April 30, 2020

First decision: May 15, 2020

Revised: July 27, 2020

Accepted: August 15, 2020

Article in press: August 15, 2020

Published online: September 14, 2020

P-Reviewer: Altonbary AY, Elkholly SE, Fusaroli P

S-Editor: Zhang L

L-Editor: Webster JR

METHODS

PVA hydrogel (Sigma Aldrich, degree of hydrolysis 99%) for simulating EUS/EUS-E lesions was investigated in Unidad de Investigación y Desarrollo Tecnológico at Hospital General de México “Dr. Eduardo Liceaga”, Mexico City. We evaluated physical, contrast, elasticity and deformation coefficient characteristics in lesions, applying Kappa’s concordance and satisfaction questionnaire (Likert 4-points).

RESULTS

PVA hydrogel showed stable mechanical properties. Density depended on molecular weight (MW) and concentration (C). PVA blocks with the greatest density showed lowest tensile strength ($r = -0.8$, $P = 0.01$). Lesions were EUS-graphically visible. Homogeneous and heterogeneous examples were created from PVA blocks or PVA phantoms, exceeding ($MW_2 = 146000-186000$, $C_9 = 15\%$ and $C_{10} = 20\%$) with a density under ($MW_1 = 85000-124000$, $C_1 = 7\%$ and $C_2 = 9\%$). We calculated elasticity and deformation parameters of solid (blue) areas, contrasting with the norm (Kappa = 0.8; high degree of satisfaction).

CONCLUSION

PVA hydrogels were appropriate for simulating organs and digestive lesions using EUS/EUS-E, facilitating practice and reducing risk. Repetition amplified skills, while reducing the learning curve.

Key Words: Endoscopic ultrasound simulators in endoscopy; Polyvinyl alcohol; Endoscopic ultrasound; Endoscopic ultrasound elastography; Strain; Elasticity

©The Author(s) 2020. Published by Baishideng Publishing Group Inc. All rights reserved.

Core Tip: Endoscopic ultrasound (EUS)/EUS-elastography simulation reduces the learning curve. In this study, the mechanical properties of polyvinyl alcohol (PVA) hydrogel were standardized to simulate digestive organs and lesions. PVA hydrogels with stable mechanical properties were obtained; the density depended on the molecular weight (MW) and concentration (C), and the PVA hydrogels with the highest density showed less tensile strength. All lesions were visible by EUS/EUS-elastography; those that were homogeneous and heterogeneous were created with hydrogels of higher density (MW_2 , C_9 and C_{10}) and lower density (MW_1 , C_1 and C_2), respectively. In conclusion, PVA hydrogels are appropriate for simulating organs and digestive lesions, facilitating practice and reducing risk.

Citation: Galvis-García ES, Sobrino-Cossio S, Reding-Bernal A, Contreras-Marín Y, Solórzano-Acevedo K, González-Zavala P, Quispe-Siccha RM. Experimental model standardizing polyvinyl alcohol hydrogel to simulate endoscopic ultrasound and endoscopic ultrasound-elastography. *World J Gastroenterol* 2020; 26(34): 5169-5180

URL: <https://www.wjgnet.com/1007-9327/full/v26/i34/5169.htm>

DOI: <https://dx.doi.org/10.3748/wjg.v26.i34.5169>

INTRODUCTION

According to the American Society for Gastrointestinal Endoscopy, before trainees can be certified in advanced endoscopic techniques, they must perform a minimum number of procedures to achieve competence^[1]. Simulators may reduce the learning curve^[1]; however, current models do not recreate reality, require considerable investment in terms of time and resources, and do not necessarily reproduce the haptic^[2,3]. Biomaterials, compatible with human tissues make it possible to simulate lesions^[4]. Natural (collagen, chitosan, fibrin, *etc.*) or synthetic hydrogels [polyethylene oxide, polyacrylic acid, polyvinyl pyrrolidone and polyvinyl alcohol (PVA)], absorb liquid without dissolving, due to their permeability and low friction coefficient^[5,6]. Manipulation of the molecular weight (MW) and concentration of the PVA hydrogel results in contrasting densities (viscoelasticity), in order to simulate models more realistically^[7-9]. These phantoms are compatible with magnetic resonance imaging and

P-Editor: Ma YJ



ultrasonography; which can produce acoustic, optical and elastographic images^[10]. Elastography measures the degree of tissue stiffness illustrated in digital color distribution by means of the deformation histogram (DH) and strain ratio (SR). The classification system for EUS-elastography (EUS-E) is based on color patterns that measure the degree of tissue stiffness. EUS-E refers to the region of interest: A which comprises the tumor area and B the soft surface quotient; B/A strain ratio (SR) represents the elastographic measurement of interest^[11-13]. Lee *et al*^[14] reported the DH effectiveness for diagnosing solid masses is 97.7%. The sensitivity (SR > 6.04 or elasticity < 0.05%) and specificity (SR > 15.41 or elasticity < 0.03%) of the SR is close to 100%. However, these results were not confirmed with the same high figures in subsequent studies^[15-17].

Although results are not consistent, knowledge of elasticity coefficient of digestive organs and lesions (cystic, semi-solid and solid) makes it possible to create more realistic models, due to the viscoelastic properties of PVA hydrogels. It is thus important to assess the modulus of elasticity or Young's modulus ($E = \text{stress}/\text{strain}$; KPa) of phantoms in order to construct them and compare them with tissues^[18]. This work was designed to standardize the mechanical properties of PVA phantoms, employing endoscopic ultrasound images for the simulation of organs and digestive lesions and elastography to evaluate the degree of tissue stiffness.

MATERIALS AND METHODS

This experimental study was performed in the Unidad de Investigación y Desarrollo Tecnológico (its acronym in Spanish is Unidad de Investigación y Desarrollo Tecnológico) of Hospital General de México "Dr. Eduardo Liceaga", Mexico City. PVA hydrogels (phantoms) with different densities (by changing molecular weight and concentration) were prepared. The study was exempt from approval by the Ethics Committee as there are no live specimens involved (human or animal tissue). Two molecular weights were used: $MW_1 = 85000-124000$ and $MW_2 = 146000-186000$ and a range of PVA concentrations: 3%, 5%, 7%, 9%, 12%, 15% and 20% (Sigma-Aldrich) with a 99.9% degree of hydrolysis.

Preparation of PVA phantoms

We used the following equation to obtain the desired concentrations of PVA phantoms (3%, 5%, 7%, 9%, 12%, 15% and 20%) for the two molecular weights, and to calculate the weight of PVA powder in 100 mL of Milli-Q ultrapure H_2O (Merck). The PVA powder crystals were dissolved after heating the mixture to 90°C, while stirring continuously (magnetic bar) until a more homogeneous hydrogel was obtained. The hydrogel was cooled for 25 min at room temperature (25°C) and stored in stainless steel boxes (containers) to avoid contamination and ensure accuracy in terms of dimensions, as presented in [Figure 1](#). The containers were subjected to four freezing cycles (-80°C/1.5 h; Freezer-Kaltis) and defrosting (25°C/4 h), until the phantoms showed stable mechanical properties. They were then submerged in ultrapure water for preservation (where they can last for years).

Density and Young's modulus

The density (g/cm^3) and Young's modulus (elasticity module, KPa) for each phantom ($E = \text{stress}/\text{strain}$) were calculated after trimming the films (1 cm × 1 cm × 0.2 cm) from the PVA phantoms.

Endoscopic ultrasound images

Images were obtained (Olympus GF-UM160 and Pentax Medical EUS 360° EG-3670URK), after submerging the phantom (Milli-Q ultrapure water at 25°C) and pressing one of its walls with a latex balloon, placed on the tip of the echoendoscope, as presented in [Figure 2](#).

The frequency used was 7.5 MHz. Images were contrasted to those of healthy organs (pancreas and liver) and pancreatic lesions (cysts and solid masses).

Endoscopic ultrasound elastography images

We evaluated phantoms in terms of stiffness/elasticity (Pentax EUS-Hitachi EUB900, Real-Time Tissue Elastography) with 2-panel images in *B* mode of conventional grayscale (right) and elastographic image (left). The frequency used was 7.5 MHz (5.0 to 10.0 MHz)^[19]. The point of interest (A or B) was measured to determine the degree of normal deformity (SR) < 6.04 and the degree of normal elasticity (B/A ratio) > 0.05%.

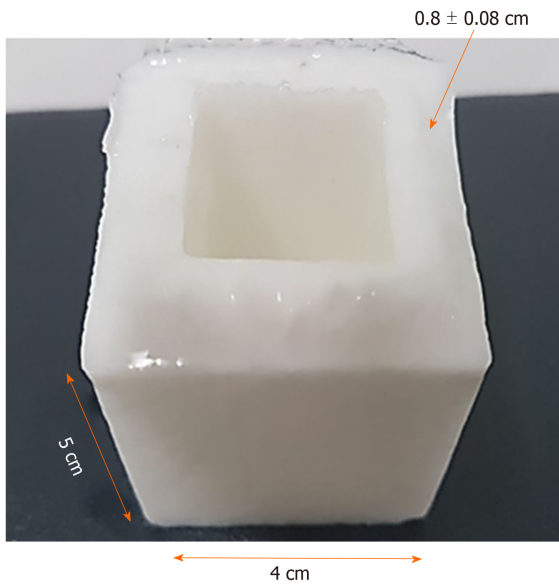


Figure 1 Stainless steel mold used to obtain polyvinyl alcohol phantoms.

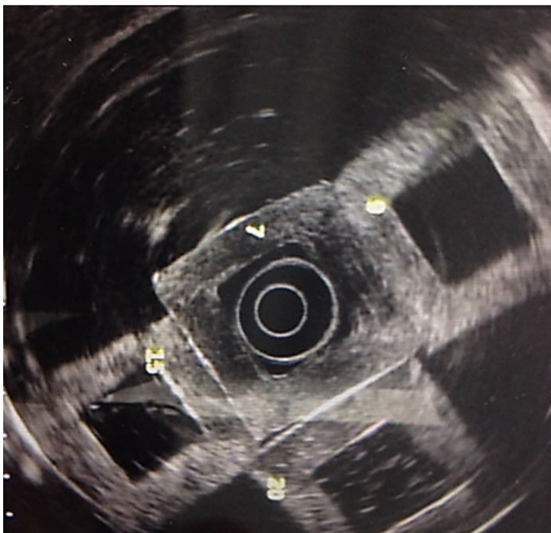


Figure 2 Endoscopic ultrasound images with the echoendoscope placed inside the polyvinyl alcohol phantom.

The “A” area comprises the largest area of the tumor and the “B” area the soft surface (red). The B/A ratio (strain ratio) was considered to represent an elastographic evaluation^[12].

Observers

Observer 1 had > 12 years of experience in EUS diagnosis, with formal training in Denmark and Venezuela, and was in charge of the area in the HGM; Observer 2 had > 8 years of experience in EUS diagnosis, with formal training in Mexico and the United States.

Statistical analysis

We calculated the inter-observer agreement (kappa index, intra-class correlation coefficient, and extent of agreement) between the two EUS experts. To compare their congruence, we conducted an independent and blind test of simulated/real images. Kappa values and degree of concordance were as follows: < 0.2 = Poor, 0.21-0.40 = Weak, 0.41-0.60 = Moderate, 0.61-0.80 = Good, and 0.81-1.00 = Very good.

A satisfaction survey was applied, consisting of nine questions regarding the simulated image (Likert-4 points: 0 = Not satisfied, 1 = Little satisfied, 2 = Quite satisfied and 3 = Very satisfied): (1) Normal pancreas; (2) Normal liver; (3)

Homogeneous lesions; (4) Heterogeneous lesions; (5) Solid lesions; (6) Cystic lesions; (7) Semi-solid lesions; (8) Elastographic image contrast; and (9) Feasibility of measuring the degree of elasticity. For the analysis, the measurement was binary (22 table): Yes = Very satisfied/satisfied *vs* No = Moderately satisfied/not satisfied, and 20 images were evaluated. The correlation between density and degree of elasticity of tissues was calculated.

RESULTS

The density and Young's modulus (M.Y.) of each PVA-phantom are summarized in [Table 1](#). The stiffness of the phantom was correlated with higher MW and concentration (correlation $r = 0.8$, $P = 0.01$) and with the increase in density and M.Y. This depended on cross-linking the monomers by freeze/thaw cycles. Simulated lesions were visible using EUS. As shown in [Figure 3](#), endoscopic ultrasound revealed differences between phantoms: C_1 *vs* C_5 ($MW_1 = 85000$ - 124000).

Density was higher in homogeneous lesions ($MW_2 = 146000$ - 186000 : $C_9 = 15\%$ and $C_{10} = 20\%$), ([Figure 4](#)) than in heterogeneous lesions ($MW_1 = 85000$ - 124000 : $C_1 = 7\%$ and $C_2 = 9\%$) ([Figure 5](#)). Concordance was 0.8 with a high degree of satisfaction.

Cystic lesions were created with higher density phantoms: C_6 and C_{10} ($MW_2 = 146000$ - 186000) ([Figure 6](#)). These cystic lesions were measured by EUS (E-EUS was never used for this). Concordance was 0.8 (kappa), with a high degree of satisfaction (Likert scale 4-points). Solid lesions were contrasted with soft areas ([Figure 7](#)). The color contrasts, RI: A and B, and SR: B/A of elastographic images are presented in [Figure 8](#). We observed lower elasticity (dark blue area), in the case of a simulated solid lesion that contrasted with green areas (normal). SR values of > 6.04 or elasticity of $< 0.05\%$ corresponded to areas with less elasticity (rigid). The differences between the B/A ratios (65.6 *vs* 7.13) and point A (0.02 *vs* 0.07%) translated into greater tissue stiffness. [Figure 9](#) and [Table 2](#) show the relationship between points of interest and strain ratios with different PVA phantom densities.

DISCUSSION

Simulation by EUS/EUS-E of visible organs and lesions is feasible using PVA phantoms. The model had high inter-observer concordance and satisfaction. This simulation facilitates practice, while curtailing risk. The increase in the number of repetitions amplifies skills and reduces the learning curve^[2,3]. However, the models lack the realism necessary to achieve competence^[2]. The focus of our experiment was to build lesions and organs visible by EUS and EUS-E, but we did not evaluate whether the technique was the most appropriate tool for differentiating malignant lesions from normal tissue. We were able to create realistic ultrasonic images using PVA phantoms. However, knowledge of the elastographic parameters of different tissues allowed us to create simulated lesions due to the viscoelastic properties of the PVA hydrogel and to contrast these with normal structures. EUS-E enables a comparison between the target and normal tissue but a stiff lesion can be either benign or malignant; therefore, the elastic properties of a tumor area may be different to those in another area^[15]. Currently, the effectiveness of the DH for diagnosing solid masses is a matter of debate and outcomes are controversial. However, the rationale for using EUS-E in chronic pancreatitis relates to the possibility of detecting the increased degree of fibrosis in diseased pancreas, compared to normal pancreas^[19]. Despite the controversy, we selected the B/A ratio (strain ratio) to measure tissue stiffness^[12] as well as the region of interest. A and B were marked in different colors (on a scale of 0-255)^[19]. It is difficult to place the region of interest of the target at the same level; this is associated with low specificity and reproducibility, and great variability in cutoff for inflammatory pancreatic masses and pancreatic cancer^[15]. In contrast, if the lesion appears soft, EUS-E can rule out malignancy with a high level of certainty. However two negative fine needle aspirations (FNAs), using EUS, in the case of a soft and enhancing lesion can rule out the diagnosis of pancreatic adenocarcinoma in 95% of patients^[15]. The accuracy of strain ratio to distinguish between normal pancreas and pancreatitis is greater, but depends on the cutoff (97.7%-ROC 0.98^[19] and 91%^[18]). However, one of the largest single-center studies reported a modest diagnostic utility by quantitative analysis (4.65 for SR and 0.27% for mass elasticity) for discriminating pancreatic masses^[17]. One analysis of the qualitative pattern for diagnosing malignancy reported 94% accuracy (ROC curve 0.854, $P < 0.0001$)^[20] with high interobserver coincidence (0.77 and 0.84,

Table 1 Relationship between Young's Modulus and different densities of polyvinyl alcohol phantoms

Molecular weight	Concentration	ρ (g/cm ³) ¹	M. Y (KPa) ¹
MW ₁ = 85000-124000	C ₁ = 7%	0.84 ± 0.11	380 ± 0.63
	C ₂ = 9%	0.92 ± 0.07	518 ± 0.50
	C ₃ = 12%	0.96 ± 0.13	780 ± 0.28
	C ₄ = 15%	1.43 ± 0.63	910 ± 0.23
	C ₅ = 20%	1.46 ± 0.18	1050 ± 0.20
MW ₂ = 146000-186000	C ₆ = 7%	0.91 ± 0.08	395 ± 0.23
	C ₇ = 9%	0.97 ± 0.11	525 ± 0.20
	C ₈ = 12%	1.22 ± 0.24	798 ± 0.18
	C ₉ = 15%	1.46 ± 0.22	922 ± 0.13
	C ₁₀ = 20%	2.08 ± 0.50	1120 ± 0.10

¹The data for ρ and M.Y (Young's modulus) are the average of four measurements of each phantom.

Table 2 Strain ratios (B/A) and regions of interest: A and B

Strain ratios (B/A)				
A	B	C	D	E
0.1	93.3	23	0.04	0.12
A 0.81	0.1	0.2	0.41	0.13
B 0.01	0.9	0.42	0.02	0.02
F	G	H	I	J
30.18	69.67	34.5	254.3	7.0
A 0.05	0.02	0.03	0.01	0.04
B 1.57	1.64	1.05	2.33	0.3

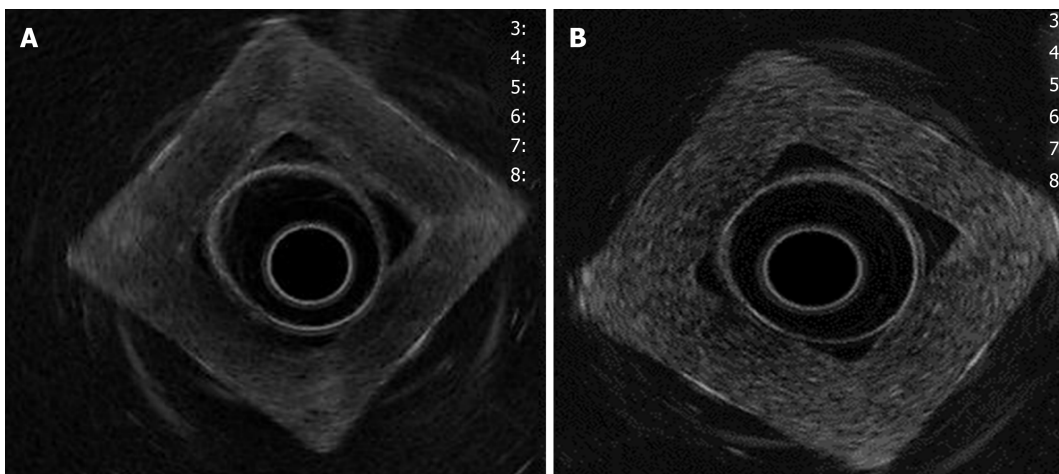


Figure 3 Comparison of endoscopic ultrasound images: A: Phantom concentration 1; B: Phantom concentration 5.

respectively)^[20,21]. By using quantitative analysis, bias in selecting the target was diminished (accuracy 89.7%)^[17].

Furthermore, multilayer perceptron neural networks can be trained to classify focal lesions as either benign or malignant (accuracy 95%)^[21]. Our phantom was designed to distinguish lesions, increase the n (repetitions), and evaluate skills for selecting a

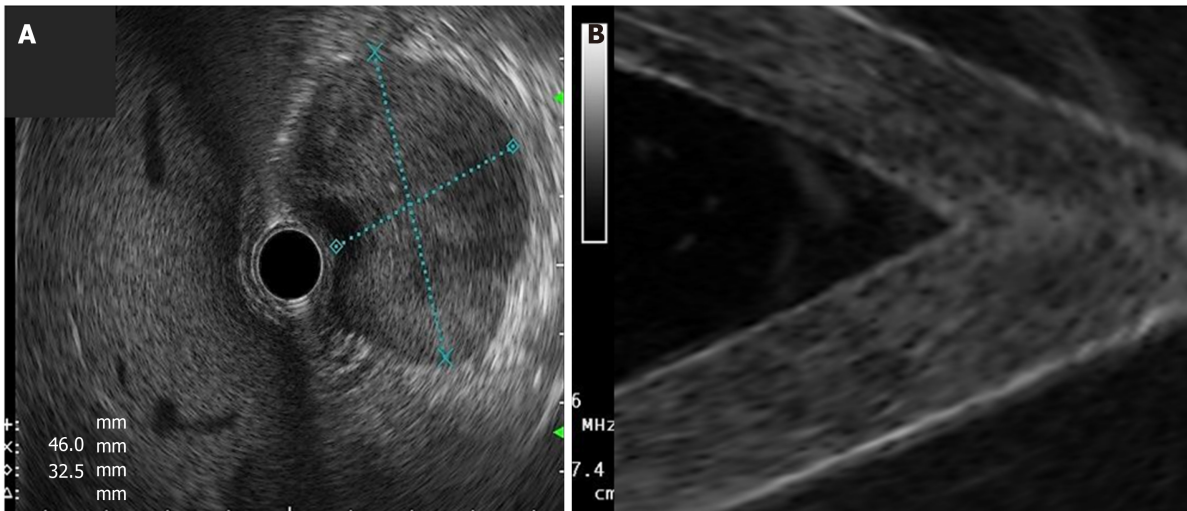


Figure 4 Type of lesions: A: Real homogeneous; B: Simulated homogeneous that refers to the liquid component inside the polyvinyl alcohol (PVA) phantom (blue arrow), surrounded by 15% PVA (concentration 9) and 20% PVA (concentration 10).

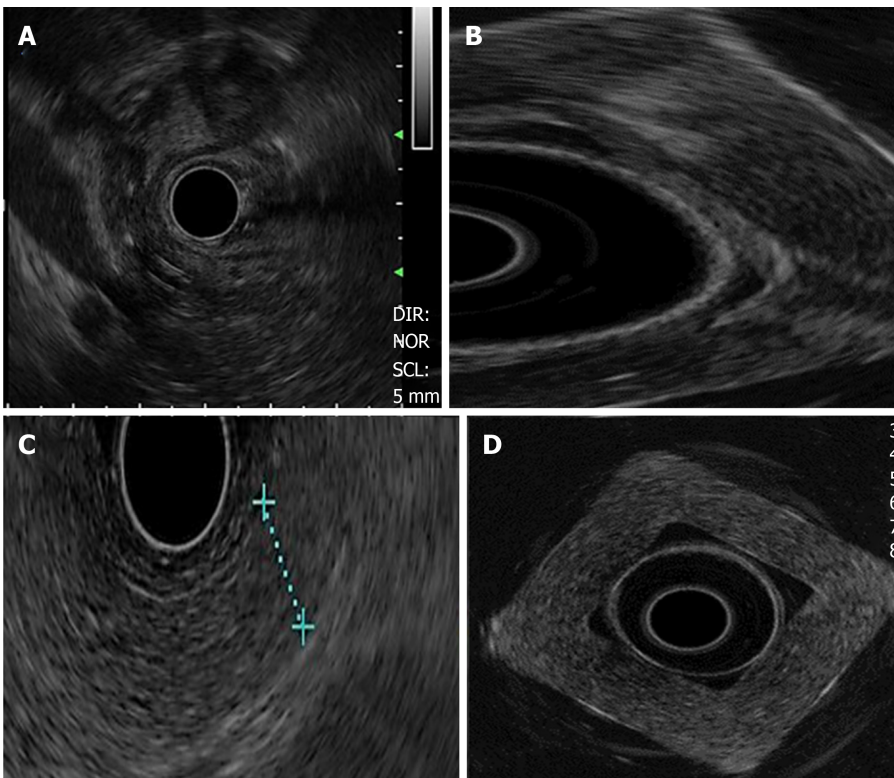


Figure 5 Type of lesions: A: Real heterogeneous lesion; B: Simulated heterogeneous lesion of hypoechoic predominance (concentration 1); C: Normal pancreatic tissue; and D: Simulated homogeneous image: phantom with 20% polyvinyl alcohol (concentration 10).

target, while improving spatio-temporal and haptic skills. A great advantage of practice with our phantom is that there is no need to practice EUS/EUS-E exclusively on animals. Qualitative pattern analysis yielded a high accuracy of 92.9% (ROC: 0.95) for the differential diagnosis between benign and malignant lymph nodes (LNs)^[22]. The accuracy for discriminating between these is of great importance for prognosis and selection of appropriate therapy^[23]. Due to the characteristics of LNs, these can also be simulated using our phantom. Another study reported lower yield of EUS-E (strain ratio) in detecting LNs but prevalence was greater (61%) in 34 patients, and it showed great heterogeneity (large width of the 95% confidence intervals)^[24]. Learning in clinical scenarios in order to acquire skills has ethical and legal implications. The low prevalence of cases is a severe limit to training, in addition to the fact that in most

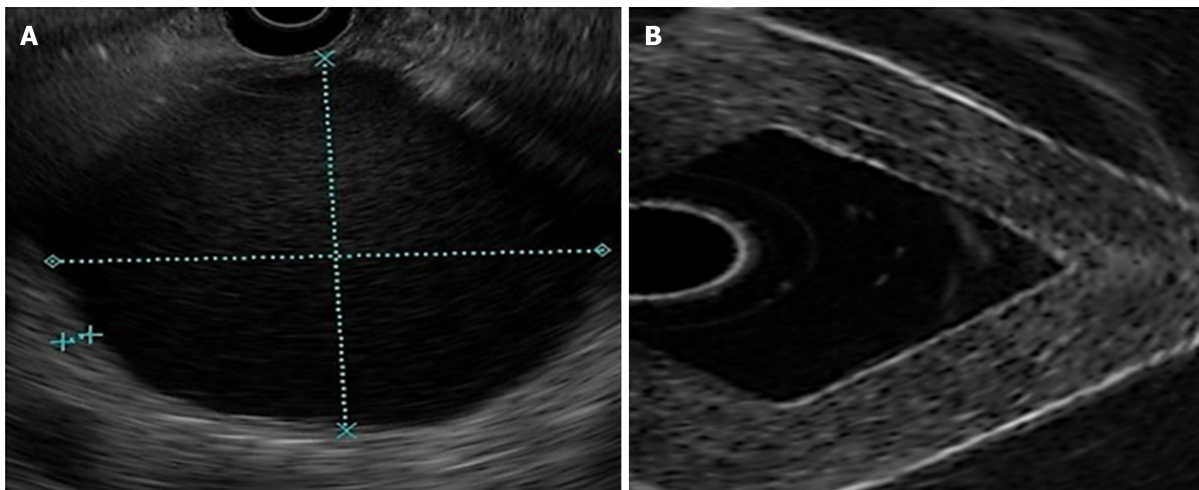


Figure 6 Cystic lesion: A: A hypoechoic image surrounded by a hyperechoic wall is visible, which produces a posterior reinforcement compatible with a pseudocyst of the pancreas (real image); and B: Endoscopic ultrasound contrast of the interior and exterior of the polyvinyl alcohol phantom (concentration 10): A hypoechoic image (inside) surrounded by a hyperechoic image (wall).

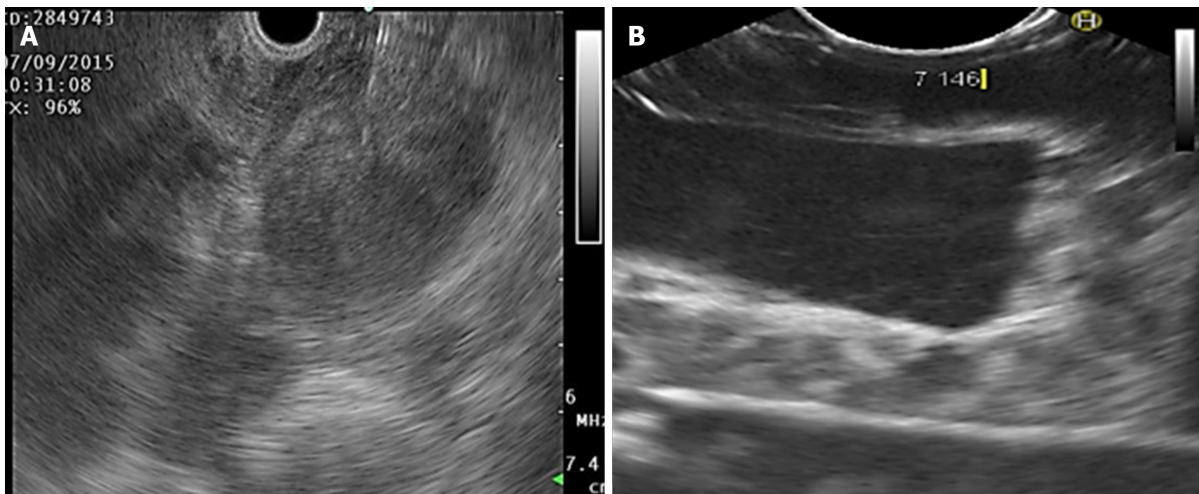


Figure 7 Solid lesion: A: Real; and B: Simulated (concentration 10).

centers, it is the expert who performs the interventions^[1]. Regarding biomaterials, these have been used to obtain acoustic, optical and elastographic images^[8,11,12,18]. In order to have greater realism in our simulated lesions, we needed to assess the mechanical properties (elasticity/stiffness) of tissue. In our experiment, biomaterial concentration was inversely proportional to the degree of tissue elasticity. The retention of liquid within the fibers produces echogenic differences. If we increase the density of the biomaterial, it will tend to be more homogeneous and hyperechoic. Density disperses sound and modifies impedance^[16].

In our study, density manipulation made it possible for us to build more realistic models. The presence of bubbles within the material increased the degree of realism. The degree of water retention within the phantoms enables the simulation of different injuries. The 20% concentrations (C_5 and C_{10}) contain less water (solid lesions), in contrast to those at 7% (C_1 and C_6), which contain a greater quantity (semi-solid). PVA characteristics are dynamic and differ when densities are compared. The area of least elasticity ($> M.Y$) is the point of greatest strength and cross-linking. The zone of least tension is the place where the transducer exerts pressure (deformity). The advantages of using PVA phantoms are as follows: (1) They do not require different equipment to that commonly used for patients, however, for the animal model they do; (2) Organs and lesions, whether hard or soft, can be simulated by modifying the molecular weight, concentration and freeze/thaw cycles of PVA; and (3) The simulators are inexpensive, this will vary depending on the size and sophistication of the phantom, for example depending on the completeness of an organ. In this work, as it only

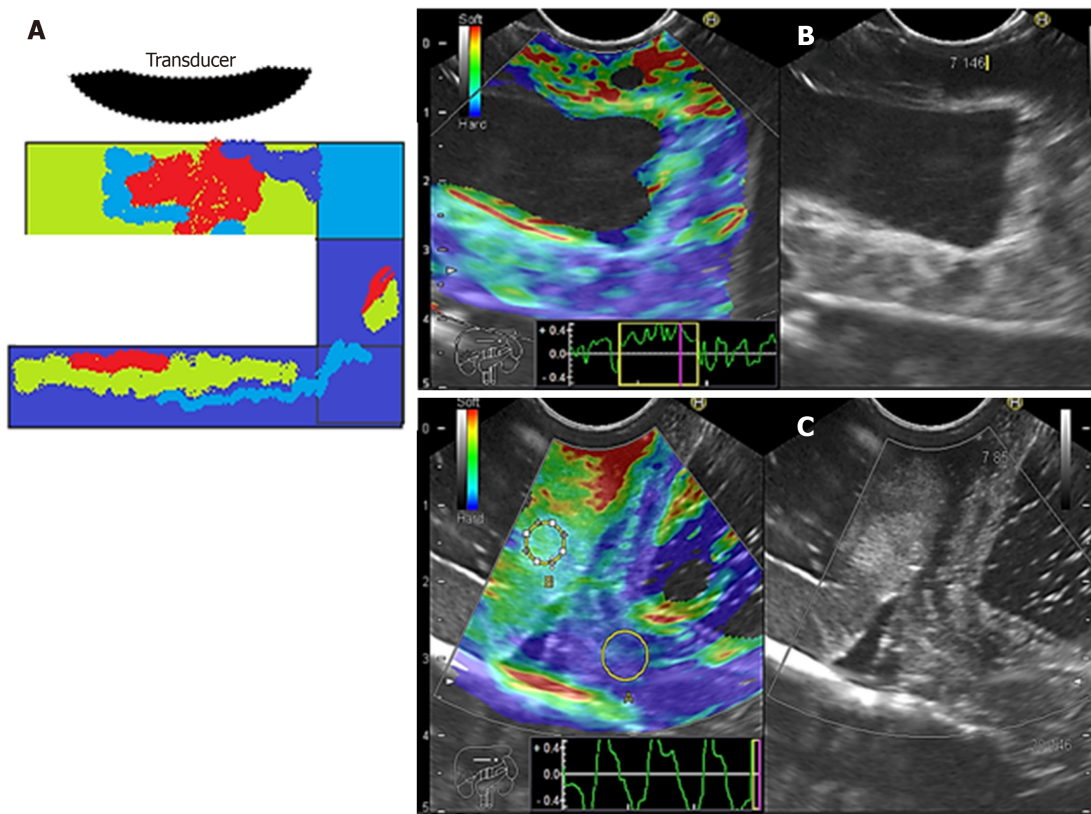


Figure 8 Elastographic images. A: Diagram showing color distribution; B: Color scale (elastography) of phantom concentration (C) 6; and C: Contrast between phantom C₆ (green hue) molecular weight 2 = 146000– 186000 vs phantom C₅ (dark blue hue) with molecular weight 1 = 85000 – 124000.

consisted of phantom characterization, each phantom costs approximately \$15 to \$20; 4) phantoms can be reused many times, provided they are kept immersed in water at room temperature (25-27°C) after use. Limitations in this study include: (1) It is necessary to submerge the PVA phantom in the water container; and (2) The main problem with EUS-E refers to difficulties in controlling tissue compression by the EUS transducer that may increase errors in measurement. Knowledge of the elasticity coefficient made it possible to create solid and semi-solid organs; both homo and heterogeneous, as well as more realistic cystic and solid lesions, due to the advantages of the viscoelastic properties of the phantom.

CONCLUSION

In conclusion, the use of PVA phantoms with different densities allowed adequate and consistent simulation of organs and digestive lesions, visible by EUS-E.

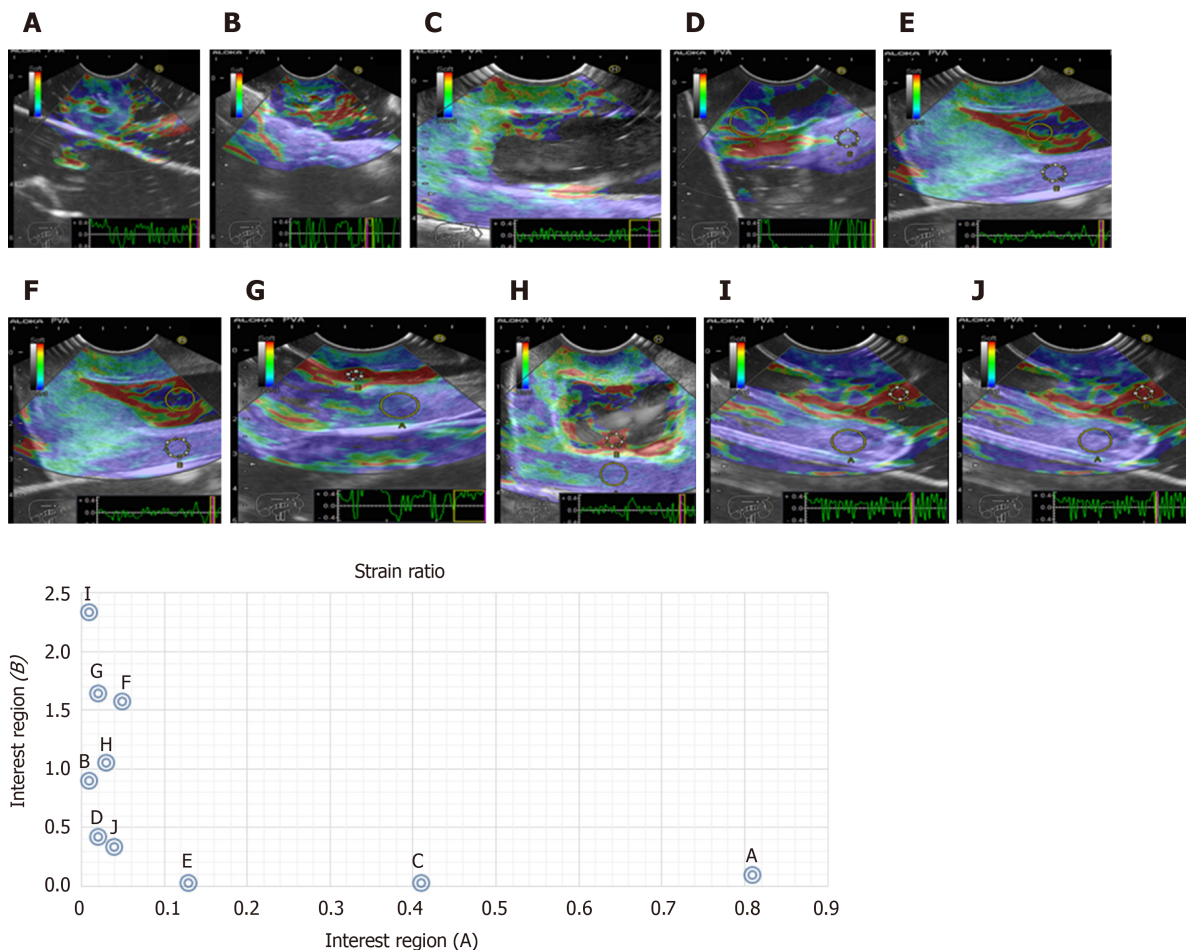


Figure 9 Relationship between the region of interest A and B and the (B/A) strain ratio.

ARTICLE HIGHLIGHTS

Research background

Training endoscopy by simulation facilitates practice while curtailing risk. However, the models lack realism to achieve competence. In order to have greater realism in simulated lesions, it is important to know the mechanical properties (elasticity /stiffness) of polyvinyl alcohol (PVA) hydrogels.

Research motivation

According to the American Society for Gastrointestinal Endoscopy, before trainees can be certified in advanced endoscopic techniques, they must perform a minimum number of procedures to achieve competence. It is important that endoscopic simulators recreate reality, but most do not, and require considerable investment in terms of time and resources, and do not necessarily reproduce the haptic. We need to build phantoms that recreate reality.

Research objectives

This study was designed to standardize the mechanical properties of PVA phantoms, using endoscopic ultrasound (EUS) images to simulate organs and digestive lesions, and Endoscopic Ultrasound Elastography (EUS-E) to evaluate the degree of tissue stiffness.

Research methods

PVA phantoms with different densities were prepared by changing the molecular weight (MW) and concentration (C). Ultrasound images of these phantoms were obtained to contrast them with healthy organs and digestive lesions. Stiffness/elasticity with 2-panel images in B mode of conventional grayscale (right) and an elastographic image (left) were evaluated. Two observers qualified all

EUS/EUS-E images (Kappa index).

Research results

The density of PVA phantoms depended on MW and C. The stiffness of these phantoms was correlated with higher MW and C (correlation $r = 0.8$, $P = 0.01$) as well as with increasing density and M.Y. All simulated lesions were visible using EUS. We calculated elasticity and deformation parameters of solid (blue) areas, contrasting with the norm (Kappa = 0.8; high degree of satisfaction)

Research conclusions

The use of PVA phantoms with different densities allowed adequate and consistent simulation of organs and digestive lesions, visible by EUS/EUS-E. Knowledge of the elasticity coefficient made it possible to create different lesions.

Research perspectives

Training in a clinical setting has medical and legal implications. Skill and abilities depend on shortening the learning curve. However, in order to achieve this, a model must be realistic. PVA phantoms were demonstrated to be feasible, economical and realistic models for EUS/EUS-E training.

ACKNOWLEDGEMENTS

To Dr. Jorge Cerecedo-Rodríguez (Hospital Ángeles Acoxpa) for his contribution to the interpretation of the endosonographic images. Thanks to the engineers Yair Pacheco, Javier Márquez Cortez (Medical Scope) and Lilia Vázquez Romero (Endomédica, S.A. de C. V) for informing us about the technical aspects of obtaining EUS/elastography images.

REFERENCES

- 1 **ASGE Training Committee**. DiMaio CJ, Mishra G, McHenry L, Adler DG, Coyle WJ, Dua K, DeGregorio B, Enestvedt BK, Lee LS, Mullady DK, Pais SA, Rajan E, Sedlack RE, Tierney WM, Faulx AL. EUS core curriculum. *Gastrointest Endosc* 2012; **76**: 476-481 [PMID: 22898403 DOI: 10.1016/j.gie.2012.04.437]
- 2 **Gonzalez JM**, Cohen J, Gromski MA, Saito K, Loundou A, Matthes K. Learning curve for endoscopic ultrasound-guided fine-needle aspiration (EUS-FNA) of pancreatic lesions in a novel ex-vivo simulation model. *Endosc Int Open* 2016; **4**: E1286-E1291 [PMID: 27995190 DOI: 10.1055/s-0042-118176]
- 3 **van der Wiel SE**, Küttner Magalhães R, Rocha Gonçalves CR, Dinis-Ribeiro M, Bruno MJ, Koch AD. Simulator training in gastrointestinal endoscopy - From basic training to advanced endoscopic procedures. *Best Pract Res Clin Gastroenterol* 2016; **30**: 375-387 [PMID: 27345646 DOI: 10.1016/j.bpg.2016.04.004]
- 4 **Stammen JA**, Williams S, Ku DN, Guldberg RE. Mechanical properties of a novel PVA hydrogel in shear and unconfined compression. *Biomaterials* 2001; **22**: 799-806 [PMID: 11246948 DOI: 10.1016/S0142-9612(00)00242-8]
- 5 **Nugent MJ**, Higginbotham CL. Preparation of a novel freeze thawed poly (vinyl alcohol) composite hydrogel for drug delivery applications. *Eur J Pharm Biopharm* 2007; **67**: 377-386 [PMID: 17398082 DOI: 10.1016/j.ejpb.2007.02.014]
- 6 **Mirolawa EF**, Agnieszka P, Wojciech S, Krzysztof JK. Morphology assessment of chemically modified and cryostructured poly (vinyl alcohol) hydrogel. *Eur Polymer J* 2007; **43**: 2035-2040 [DOI: 10.1016/j.eurpolymj.2007.02.024]
- 7 **Wan WK**, Campbell G, Zhang ZF, Hui AJ, Boughner DR. Optimizing the tensile properties of polyvinyl alcohol hydrogel for the construction of a bioprosthetic heart valve stent. *J Biomed Mater Res* 2002; **63**: 854-861 [PMID: 12418034 DOI: 10.1002/jbm.10333]
- 8 **Gholap SG**, Jog JP, Badiger MV. Synthesis and characterization of hydrophobically modified poly (vinyl alcohol) hydrogel membrane. *Polymer* 2004; **45**: 5863-5873 [DOI: 10.1016/j.polymer.2004.06.032]
- 9 **Lamouche G**, Kennedy BF, Kennedy KM, Bisailon CE, Curatolo A, Campbell G, Pazos V, Sampson DD. Review of tissue simulating phantoms with controllable optical, mechanical and structural properties for use in optical coherence tomography. *Biomed Opt Express* 2012; **3**: 1381-1398 [PMID: 22741083 DOI: 10.1364/BOE.3.001381]
- 10 **Fromageau J**, Gennisson JL, Schmitt C, Maurice RL, Mongrain R, Cloutier G. Estimation of polyvinyl alcohol cryogel mechanical properties with four ultrasound elastography methods and comparison with gold standard testings. *IEEE Trans Ultrason Ferroelectr Freq Control* 2007; **54**: 498-509 [PMID: 17375819 DOI: 10.1109/TUFFC.2007.273]
- 11 **Saftoiu A**, Vilman P. Endoscopic ultrasound elastography-- a new imaging technique for the visualization of tissue elasticity distribution. *J Gastrointest Liver Dis* 2006; **15**: 161-165 [PMID: 16802011]
- 12 **Cui XW**, Chang JM, Kan QC, Chiorean L, Ignee A, Dietrich CF. Endoscopic ultrasound elastography: Current status and future perspectives. *World J Gastroenterol* 2015; **21**: 13212-13224 [PMID: 26715804 DOI: 10.3748/wjg.v21.i47.13212]
- 13 **Itoh Y**, Itoh A, Kawashima H, Ohno E, Nakamura Y, Hiramatsu T, Sugimoto H, Sumi H, Hayashi D,

- Kuwahara T, Morishima T, Funasaka K, Nakamura M, Miyahara R, Ohmiya N, Katano Y, Ishigami M, Goto H, Hirooka Y. Quantitative analysis of diagnosing pancreatic fibrosis using EUS-elastography (comparison with surgical specimens). *J Gastroenterol* 2014; **49**: 1183-1192 [PMID: [24026103](#) DOI: [10.1007/s00535-013-0880-4](#)]
- 14 Lee TH, Cha SW, Cho YD. EUS elastography: advances in diagnostic EUS of the pancreas. *Korean J Radiol* 2012; **13** Suppl 1: S12-S16 [PMID: [22563282](#) DOI: [10.3348/kjr.2012.13.S1.S12](#)]
- 15 Ignee A, Janssen C, Arcidiacono PG, Hocke M, Möller K, Saftoiu A, Will U, Fusaroli P, Iglesias-Garcia J, Ponnudurai R, Petrone MC, Braden B, Burmester E, Dong Y, Atkinson NS, Dietrich CF. Endoscopic ultrasound elastography of small solid pancreatic lesions: a multicenter study. *Endoscopy* 2018; **50**: 1071-1079 [PMID: [29689572](#) DOI: [10.1055/a-0588-4941](#)]
- 16 Iglesias-Garcia J, Dominguez-Muñoz JE, Castiñeira-Alvarino M, Luaces-Regueira M, Lariño-Noia J. Quantitative elastography associated with endoscopic ultrasound for the diagnosis of chronic pancreatitis. *Endoscopy* 2013; **45**: 781-788 [PMID: [24019131](#) DOI: [10.1055/s-0033-1344614](#)]
- 17 Dawwas MF, Taha H, Leeds JS, Nayar MK, Oppong KW. Diagnostic accuracy of quantitative EUS elastography for discriminating malignant from benign solid pancreatic masses: a prospective, single-center study. *Gastrointest Endosc* 2012; **76**: 953-961 [PMID: [22854060](#) DOI: [10.1016/j.gie.2012.05.034](#)]
- 18 Iglesias-Garcia J, Larino-Noia J, Abdulkader I, Forteza J, Dominguez-Munoz JE. Quantitative endoscopic ultrasound elastography: an accurate method for the differentiation of solid pancreatic masses. *Gastroenterology* 2010; **139**: 1172-1180 [PMID: [20600020](#) DOI: [10.1053/j.gastro.2010.06.059](#)]
- 19 Fusaroli P, Eloubeidi MA. Endoscopic ultrasound elastography in diagnosing chronic pancreatitis: has the strain ratio found its region of interest? *Endoscopy* 2013; **45**: 789-791 [PMID: [24068587](#) DOI: [10.1055/s-0033-1344786](#)]
- 20 Săftoiu A, Vilmann P, Gorunescu F, Janssen J, Hocke M, Larsen M, Iglesias-Garcia J, Arcidiacono P, Will U, Giovannini M, Dietrich C, Havre R, Gheorghe C, McKay C, Gheonea DI, Ciurea T; European EUS Elastography Multicentric Study Group. Accuracy of endoscopic ultrasound elastography used for differential diagnosis of focal pancreatic masses: a multicenter study. *Endoscopy* 2011; **43**: 596-603 [PMID: [21437851](#) DOI: [10.1055/s-0030-1256314](#)]
- 21 Janssen J, Dietrich CF, Will U, Greiner L. Endosonographic elastography in the diagnosis of mediastinal lymph nodes. *Endoscopy* 2007; **39**: 952-957 [PMID: [18008203](#) DOI: [10.1055/s-2007-966946](#)]
- 22 Săftoiu A, Vilmann P, Hassan H, Gorunescu F. Analysis of endoscopic ultrasound elastography used for characterisation and differentiation of benign and malignant lymph nodes. *Ultraschall Med* 2006; **27**: 535-542 [PMID: [17160759](#) DOI: [10.1055/s-2006-927117](#)]
- 23 Dumonceau JM, Deprez C, Hansen PH, Janssen C, Iglesias-Garcia J, Larghi A, Vanbiervliet G, Aithal GP, Arcidiacono PG, Bastos P, Carrara S, Czakó L, Fernández-Esparrach G, Fockens P, Ginès À, Havre RF, Hassan C, Vilmann P, van Hooft JE, Polkowski M. Indications, results, and clinical impact of endoscopic ultrasound (EUS)-guided sampling in gastroenterology: European Society of Gastrointestinal Endoscopy (ESGE) Clinical Guideline - Updated January 2017. *Endoscopy* 2017; **49**: 695-714 [PMID: [28511234](#) DOI: [10.1055/s-0043-109021](#)]
- 24 Larsen MH, Frstrup C, Hansen TP, Hovendal CP, Mortensen MB. Endoscopic ultrasound, endoscopic sonoelastography, and strain ratio evaluation of lymph nodes with histology as gold standard. *Endoscopy* 2012; **44**: 759-766 [PMID: [22752891](#) DOI: [10.1055/s-0032-1309817](#)]



Published by **Baishideng Publishing Group Inc**
7041 Koll Center Parkway, Suite 160, Pleasanton, CA 94566, USA
Telephone: +1-925-3991568
E-mail: bpgoffice@wjgnet.com
Help Desk: <https://www.f6publishing.com/helpdesk>
<https://www.wjgnet.com>

